

## a0005 Tropical Meteorology: Intertropical Convergence Zone

**DE Waliser**, Jet Propulsion Laboratory, California Institute of Technology, Pasadena, CA, USA

**X Jiang**, Joint Institute for Regional Earth System Science and Engineering, University of California, Los Angeles, CA, USA

© 2014 Elsevier Ltd. All rights reserved.

### Synopsis

abspara0010

The Intertropical Convergence Zone (ITCZ) lies in the equatorial trough, a permanent low-pressure feature where surface trade winds, laden with heat and moisture, converge to form a zone of increased convection, cloudiness, and precipitation. The latent heat released in the ITCZ is critical to the atmospheric energy budget and ITCZ cloudiness provides an important contribution to the planetary albedo. The ITCZ's position, structure, and migration influence ocean–atmosphere and land–atmosphere interactions on a local scale, the circulation of the tropical oceans on a basin scale, and a number of features of the Earth's climate on a global scale.

### s0010 Introduction

p0010

One of the features that is most readily identified with the tropical atmosphere is the Intertropical Convergence Zone (ITCZ). The ITCZ lies in the equatorial trough, a permanent low-pressure feature that marks the meteorological equator where surface trade winds, laden with heat and moisture from surface evaporation and sensible heating, converge to form a zone of increased mean convection, cloudiness, and precipitation. The latent heat released in the convective cloud systems of the ITCZ is a critical component of the atmospheric energy balance, and the enhanced cloudiness associated with these cloud systems provides an important contribution to the planetary albedo. The fluxes of heat, moisture, momentum, and radiation between the atmosphere and the surface differ dramatically between the ITCZ region and the regions to the north and south of the ITCZ. Thus, the position, structure, and migration of the ITCZ play an important role in determining the characteristics of ocean–atmosphere and land–atmosphere interactions on a local scale, the circulation of the tropical oceans on a basin scale, and a number of features of the Earth's climate on a global scale.

larger its horizontal extent. This is mostly due to the development of high cirrus clouds in the outflow region of convective systems. In contrast to deep convective 'towers', which typically have horizontal scales on the order of 1–10 km and when found in isolation usually indicate young or developing convective system, cirrus clouds can appear to extend over thousands of kilometers and encompass tens or hundreds of convective towers simultaneously. Thus, the size of the various convective systems shown in [Figure 1\(a\)](#) can be influenced by their maturity and their abundance in any one area and how these factors in turn influence the development of what appears as a common cirrus cloud. Furthermore, while most cloud systems in the tropics arise from simple convective instability, likely in conjunction with synoptic wavelike disturbances inherent to the equatorial region, the organization of some systems can be influenced by low-frequency phenomena which can increase their spatial extent. For example, the larger systems in the Indian and western Pacific Ocean may be influenced by the tropical Intraseasonal Oscillation or simply be larger due to the difference in climatological conditions (e.g., sea surface temperature) between the Eastern and Western Hemispheres which is discussed below.

### s0015 Mean Structure

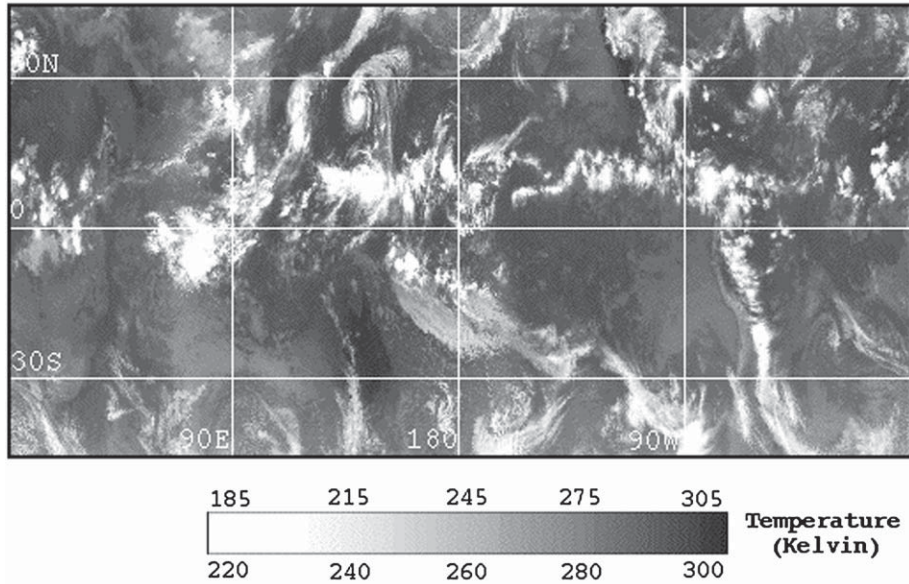
p0015

On any given day in the tropics, there are usually a number of deep convective cloud systems that appear to be somewhat randomly distributed across the equatorial region. [Figure 1\(a\)](#) shows a satellite cloud image constructed from a number of geostationary and polar orbiting satellites for 7 September 1991. Bright areas denote cold temperatures and thus in this case indicate clouds whose tops are at or near the level of the tropopause, e.g., deep convective or cirrus clouds. Dark areas denote warm temperatures, which in this case implies clear skies. Evident throughout the tropical region, and aligned roughly parallel to the equator, are a number of cloud systems. Some of these systems exhibit horizontal scales on the order of a few hundred kilometers or less. Others, such as the large system in the Indian Ocean, have horizontal dimensions on the order of about 25 000 km. The vast difference in horizontal scales of these cloud systems can arise from a number of factors. Typically, the more mature a convective system is, the

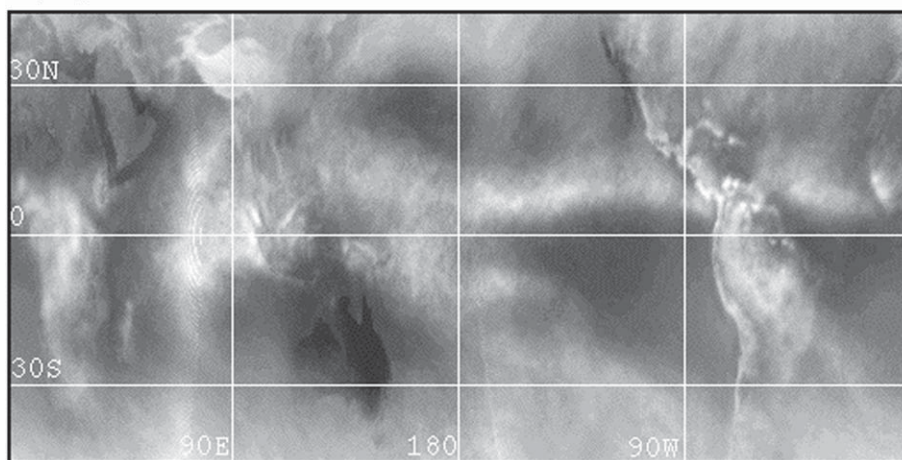
Other than the loose east–west orientation of the cloud [p0020](#) systems in [Figure 1\(a\)](#), there is no obvious systematic preference for the locations of these systems. Only upon averaging such observations over a time period relatively long (~months) compared to the lifetime of these systems (~hours–days) does a robust spatial preference become evident. [Figure 1\(b\)](#) shows a time-averaged satellite cloud image, constructed from daily cloud images, such as the one shown in [Figure 1\(a\)](#), from 1 September to 31 November 1991. From this image, it is more apparent that for a given season particular regions of the tropics are favored for the development of tropical convective systems. The spatial structure of the deep convective cloud pattern shown in [Figure 1\(b\)](#) exhibits the spatial pattern roughly identified with the ITCZ, at least for the Northern Hemisphere fall season. Thus, while the cloud (or rainfall) pattern associated with the ITCZ is usually thought of as a continuous band of clouds (or rain), at any given time, this 'band' contains only a few disparate cloud systems. [Figure 2](#) shows the long-term mean rainfall pattern. The band(s) of high rainfall represent the mean, or archetypal, ITCZ spatial structure. Overall, this structure is roughly aligned

AUT

a) September 7, 1991

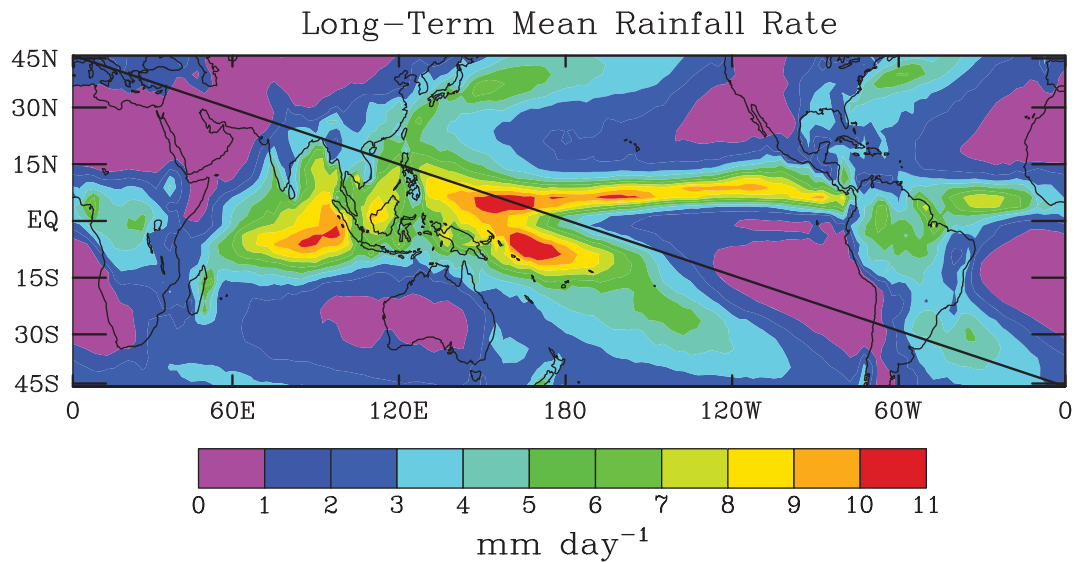
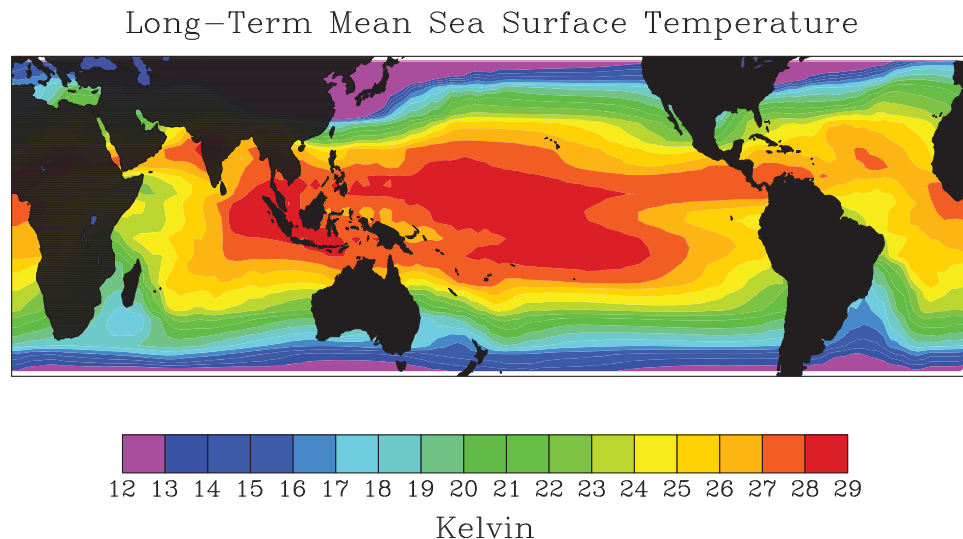


b) September-November Mean

f0010 **Figure 1**

with the equator and it exhibits a significant amount of zonal symmetry relative to the rainfall pattern in the mid-latitudes. Apart from this zonal symmetry, the ITCZ rainfall distribution displays a fair amount of longitudinal variability as well. In the Atlantic and eastern Pacific Oceans, it is made up of very narrow, intense regions of rainfall that tend to lie just north of the equator. Over the South American and African continents, the mean rainfall distribution has a considerably larger latitudinal extent and tends to lie directly over the equator. Over the eastern Indian and western Pacific Oceans, the rainfall distribution is both broad in latitude and intense in magnitude. Two of the more notable zonal asymmetries in the ITCZ are the weak rainfall over the western Indian Ocean and the southeast extension of the ITCZ over the central Pacific Ocean. The latter, referred to as the South Pacific Convergence Zone (SPCZ), leads to an area of intense rainfall on either side of the equator with a relatively dry region in between. Such a structure is often referred to as a 'double ITCZ'.

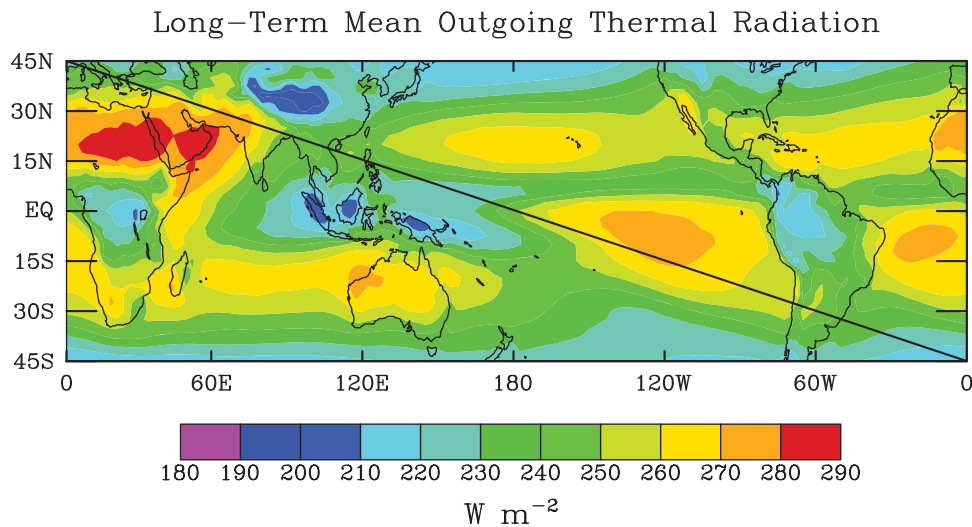
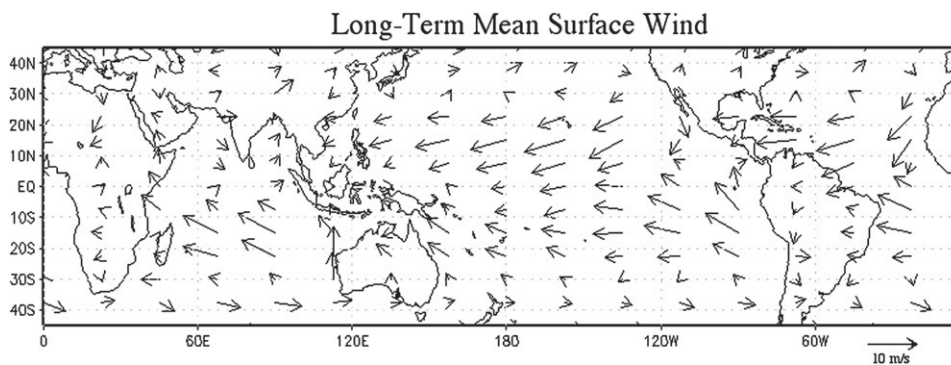
The time-mean spatial structure of the ITCZ described above <sup>p0025</sup> can be better understood by examining the time-mean sea surface temperature (SST), which is shown in [Figure 3](#). Due to the fact that on average the equatorial region receives the most solar irradiance, this region also tends to have the highest SSTs. While this tendency for very warm SST (i.e., greater than 25 °C) is mostly uniform with longitude, there are some deviations. These deviations are produced by a number of factors, including ocean basin geometry, ocean circulation properties – equatorial dynamics in particular, as well as the coupled interaction with the atmosphere, including the ITCZ itself. The relatively warm water of the equatorial region heats the air in the lower atmosphere making it less dense and buoyant relative to the air aloft. This buoyancy forcing leads to rising motion over the equatorial region. As the moist near-surface air rises, it cools adiabatically and begins to undergo condensation which releases the latent heat contained in the water vapor and produces rainfall at the surface. This latent heating enhances

f0015 **Figure 2**f0020 **Figure 3**

the buoyancy and associated upward motion of the air even further, which in turn enhances the adiabatic cooling, water vapor condensation, and surface rainfall. This process continues until nearly all the water vapor condenses out of the parcel and/or the parcel is no longer buoyant with respect to its environment. In either case, this usually happens when the parcel reaches the inversion associated with the tropopause, whereupon the air begins to move away from the equator. This divergent upper level air undergoes cooling through radiative heat loss, causing it to lose buoyancy, and sinks in the subtropical regions.

p0030 **Figure 4** shows the long-term mean outgoing thermal radiation leaving the top of the atmosphere. The regions of large radiative heat loss lie on the poleward edges of the regions of high rainfall (i.e., **Figure 2**) and extend into the subtropics.

Upon reaching the surface, this sinking air is relatively dry but gains moisture again via surface evaporation as it converges toward the equator. **Figures 5 and 6** show the long-term mean surface wind and evaporation fields. The surface wind field shows that over most of the tropical regions surface air tends to converge into the areas of high rainfall. The evaporation field indicates that as this air converges toward these equatorial regions, it gains moisture from the ocean, particularly in the areas of the 'trade winds' where the wind speeds are higher. The combination of the above processes leads to a deep meridional circulation cell, extending over the depth of the troposphere, with air converging toward the equator at low levels, rising in the equatorial regions, diverging at upper levels, and sinking in the subtropics. The zonal mean of this circulation pattern is typically referred to as the 'Hadley Circulation'.

f0025 **Figure 4**f0030 **Figure 5**

p0035 From the physical description above, it is evident that a close association exists between the spatial structure of the warmer SSTs and the rainfall pattern associated with the ITCZ. For example, **Figures 2 and 3** show that the narrow bands of rainfall over the Atlantic and eastern Pacific correspond well to the relatively warm bands of warm water north of the equator in these regions. Similarly, the very broad area of warm water in the Indian and western Pacific Oceans corresponds well to the more widespread area of intense rainfall of the ITCZ in these regions. In addition, the discussion above highlights the complex makeup of the water and energy cycles in the tropics and the role of the ITCZ within these cycles. The schematic diagram in **Figure 7** highlights important aspects of these water and energy cycles and illustrates how the physical processes associated with the ITCZ described above fit together in an idealized latitude-height diagram. The downward arrows at the top of the atmosphere depict the incoming solar energy from the sun and the fact that there is a reduction of solar energy as one moves poleward. As **Figure 1(a)** indicates, at any given time, most of the tropics exhibit clear skies. This allows a large portion of this solar energy to reach the surface and induce a pole-to-equator SST gradient, with the warmest SSTs in the near-equatorial region. The upward arrows at the surface of the

ocean depict the ocean to atmosphere energy exchange, which takes place primarily through the transfer of heat and moisture from the ocean to the near-surface air via sensible heat and latent (i.e., evaporative) heat fluxes. As the air rises over the warmest water, a convergent circulation is induced at lower levels with the upper levels exhibiting divergence. The rising air experiences adiabatic cooling which leads to condensation of the moisture and the release of the stored latent heat. The former falls back to the surface as precipitation, while the latter heats the air, leading to a further enhancement of the vertical motion. Now, the heat that was originally derived from incoming solar energy deposited in the ocean resides in the atmosphere. The upward arrows at the top of the atmosphere denote transfer of this energy back to space via radiative heat loss as the air diverges away from the equator and sinks back to the surface.

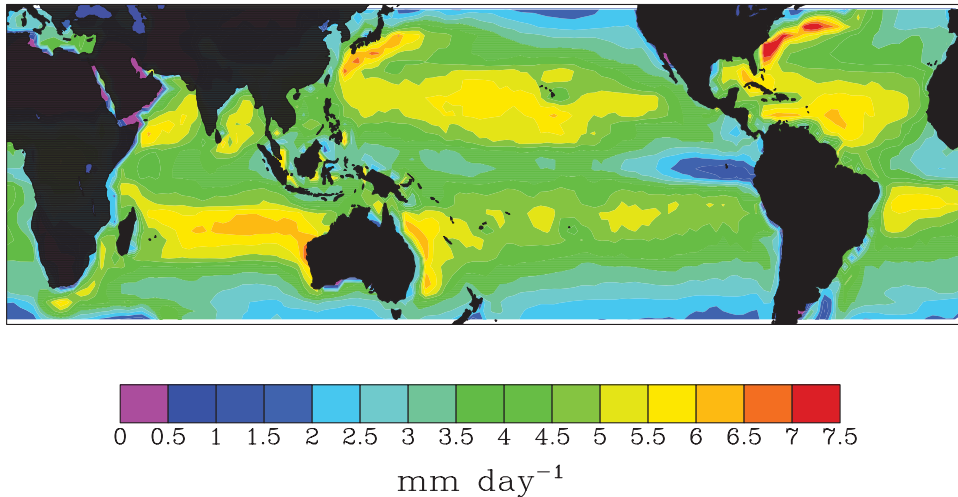
### Seasonal Variations

Over the course of the annual cycle, seasonal changes occurring in the ITCZ modify the mean structure depicted in **Figure 2**. In general, the entire line-oriented convection band marches

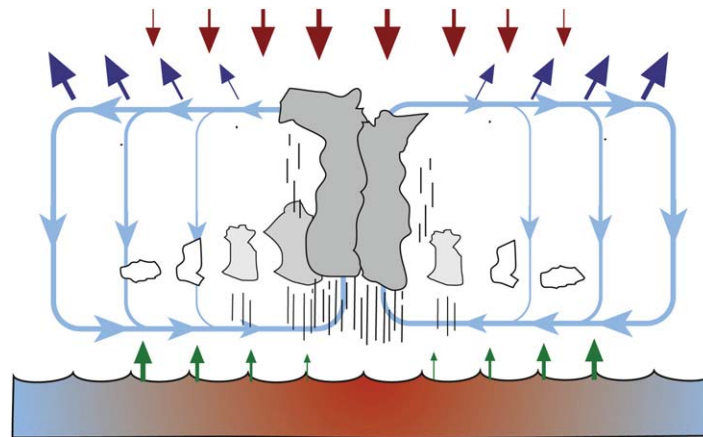
s0020

p0040

## Long-Term Mean Evaporation



f0035 Figure 6

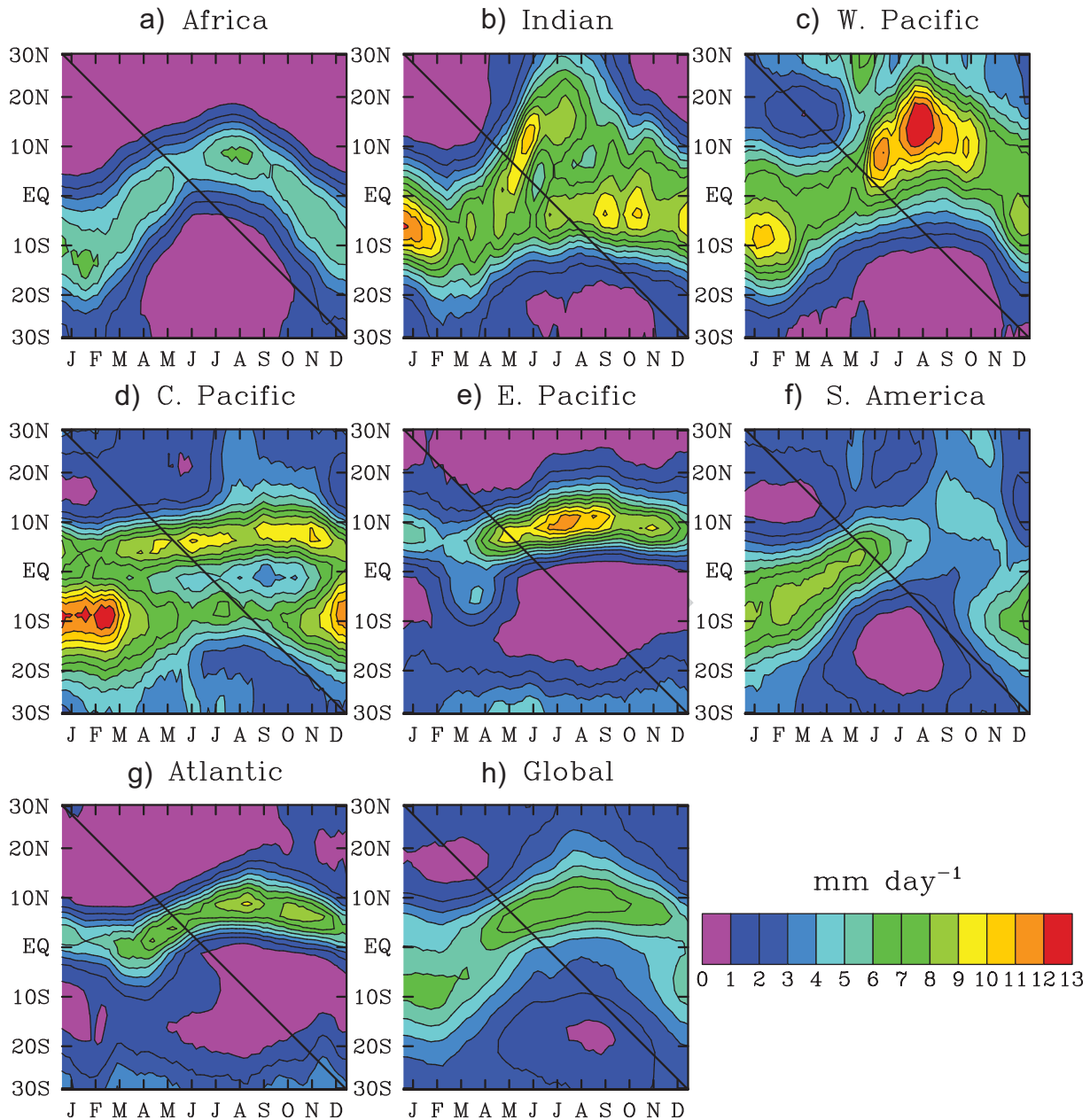


f0040 Figure 7

north in the Northern Hemisphere spring and summer and south in the Southern Hemisphere spring and summer. The differences in the amplitudes and phases of the ITCZ excursions at different longitudes are dictated in part by the different characteristics of the surface (i.e., land or ocean) and the local atmospheric circulation pattern. The ITCZ over land (e.g., Africa and South America) follows the annual march of the sun, while the migration of the ITCZ over extended ocean regions lags slightly behind by a month or two. This time lag is most apparent in the eastern Pacific and the Atlantic Oceans, where the ITCZ is furthest south in the Northern Hemisphere spring and furthest north in the Northern Hemisphere fall. The origin of this time lag is primarily due to the large thermal inertia of the ocean mixed layer compared to the land surface but also involves complex dynamical interactions that develop between the ocean and atmosphere.

p0045 While the most of the seasonal changes in the ITCZ are associated with latitudinal migration, there are other significant structural changes. One of the more significant of these is over

South America where large spatial differences exist between the 'ITCZs' of the Northern and Southern Hemisphere summers. During the Southern Hemisphere summer, the rainy season encompasses nearly the entire tropical area of the South American continent. This produces a latitudinally and longitudinally broad ITCZ. In the Northern Hemisphere summer, the ITCZ overlies the oceanic region north of the continent and has a structure more consistent with its oceanic counterparts to the east and west. Another dramatic seasonal change associated with the ITCZ occurs in the Indian Ocean region during the Asian summer monsoon. As the monsoon circulation develops and intensifies, the convection zone splits, with a very intense area of rainfall occurring over the Indian subcontinent and a weaker rainfall maximum remaining in the equatorial region. A similar intensification of rainfall occurs in the Southern Hemisphere summer over northern Australia; however, in this case, the equatorial component tends to be suppressed. During this same period, the convergence zones over Africa and the Indian Ocean become more continuous due to the reduced

f0045 **Figure 8**

coastal ocean upwelling off the east African coast. Other modest seasonal deviations occur in the eastern Pacific during the northern spring, when the ITCZ occasionally separates into two zones of convection straddling the equator. This 'double ITCZ' results from a relaxation of the southeast trade winds, which greatly diminishes the equatorial and nearby coastal ocean upwelling leaving seasonably warm surface temperatures south of the equator. In a related manner, the two branches of convergence in the central Pacific oscillate in strength during the year with the southern and northern branches intensifying during their respective summer season.

p0050 To help illustrate and quantify some of the seasonal changes in the ITCZ described above, **Figure 8** shows time-latitude

diagrams of rainfall over the course of the calendar year for a number of distinct tropical regimes. For example, **Figure 8(a)** shows that the annual cycle of the ITCZ over Africa exhibits a migration pattern that has a nearly sinusoidal nature. In this region, the ITCZ appears to closely follow the solar cycle of surface heating, with a lag of about a month. It has a fairly even intensity throughout the year ( $\sim 5 \text{ mm day}^{-1}$ ) and migrates from about 15° S to 10° N. The difference in poleward extremes is associated with the Sahara Desert, the dryness of which inhibits the northern migration of the ITCZ. In contrast to this nearly sinusoidal case, all other regions (**Figure 8(b)** and **8(g)**) show an annual cycle that has seasonal dependencies in intensity, structure, and/or a larger phase lag relative to the

solar cycle of surface heating. For example, the ITCZ migrations over the Indian (Figure 8(b)) and western Pacific (Figure 8(c)) Oceans show strong rainfall intensification associated with the summer monsoons. In particular, the Asian summer monsoon produces a significant enhancement to the rainfall in the Northern Hemisphere summer months over Southeast Asia and, as mentioned above, produces two bands of rainfall in the Indian Ocean region during this period. The annual cycle of the ITCZ in these two regions lags approximately 2 months behind the solar heating cycle.

p0055 The eastern Pacific (Figure 8(e)) and Atlantic (Figure 8(g)) Oceans have very similar annual cycles. As suggested earlier by Figure 1(b) and Figure 2, the ITCZ in these regions remains primarily in the Northern Hemisphere throughout the year, with some weak rainfall ( $\sim 4\text{--}5\text{ mm day}^{-1}$ ) occurring south of the equator in the Northern Hemisphere spring. During this time of year, warm water ( $\sim 27^\circ\text{C}$  or greater) occurs on both sides of the equator in this region and the ITCZ, in its southern most position, is split by a zone equatorial ocean upwelling (i.e., cool equatorial SSTs). The phase of the annual cycle in these regions lags behind the surface solar heating cycle by approximately 2–3 months, and each produces the most intense ITCZ in the Northern Hemisphere fall. During this season, the surface water associated with the equatorial counter-currents is warmest and the low-level trade wind convergence is strongest.

p0060 The annual cycle of the central Pacific and South America shows very different characteristics than those described above. As illustrated earlier in Figure 2, the ITCZ in the central Pacific is composed of northern and southern convergence zones straddling the equator. While this large-scale 'double' convergence zone remains intact during the course of the annual cycle, the intensity of the summer hemisphere branch tends to dominate. The annual cycle of the ITCZ over South America displays the least amount of symmetry with respect to north–south migration and ITCZ intensity. The surface underlying the ITCZ is largely responsible for this asymmetry as mentioned above. In this region, the phase of the ITCZ is locked to the annual cycle during its northward propagation. However, after having reached the oceanic region north of South America, the convection diminishes slightly, and the cycle appears to lag slightly until the rainy season begins again over the Amazon Basin in November–December. The annual cycle of the global ITCZ has a modest resemblance to a sinusoidal pattern, with the intensity of the zonally averaged mean rainfall being strongest during the Northern Hemisphere summer and fall ( $\sim 7\text{ mm day}^{-1}$ ) and weakest during the equinoxes ( $\sim 5\text{ mm day}^{-1}$ ).

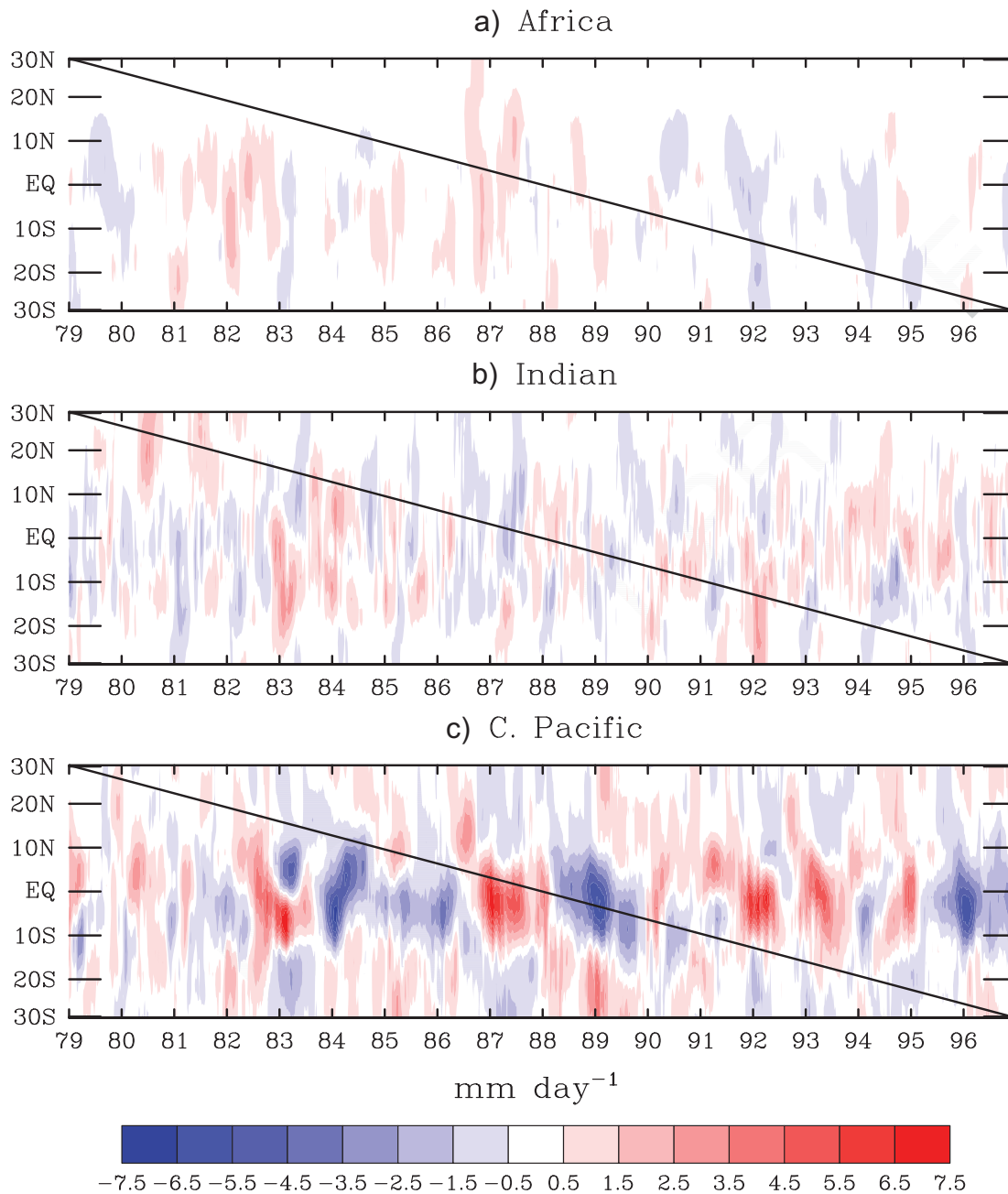
## s0025 Interannual Fluctuations

p0065 Apart from the regular seasonal variations, the ITCZ undergoes interannual fluctuations in its position and intensity. Figure 9 illustrates the range of interannual variability exhibited by the ITCZ over the period 1979–98 for three of the longitude sectors discussed in the previous section. This figure shows time-latitude diagrams of the seasonal anomalies of rainfall from the mean annual cycles presented in Figure 8. Note that each is plotted using the same color scale. Immediately evident is the

fact that the interannual anomalies in the ITCZ position and intensity are weakest over Africa and strongest for the ITCZ over the central Pacific Ocean. Typical seasonal rainfall anomalies for the ITCZ over Africa are about  $\pm 0.5\text{ mm day}^{-1}$  and range up to about  $\pm 1.5\text{ mm day}^{-1}$  in the more extreme events. Depending on the location and intensity of the mean ITCZ rainfall band, these values represent variations on the order of 10–25% of the mean values. Overall, these anomalies illustrate that this region undergoes relatively weak, low-frequency rainfall variations with the early and late 1980s being relatively wetter than normal and the late 1970s and early 1990s being relatively drier than normal. Within this low-frequency variability are periods where the ITCZ exhibits short-lived variability in its intensity and latitude. For example, during the 1981–82 winter, the ITCZ extended anomalously southward, while in the 1982–83 winter, the rainfall associated with the ITCZ was about 25% stronger than normal. During the fall of 1986 and summer of 1987, the ITCZ extended anomalously northward, bringing rain to the normally dry Sahara Desert. Another notable anomaly in the ITCZ over Africa occurred in the winter of 1991–92 when the ITCZ was particularly weak and did not migrate as far south as normal.

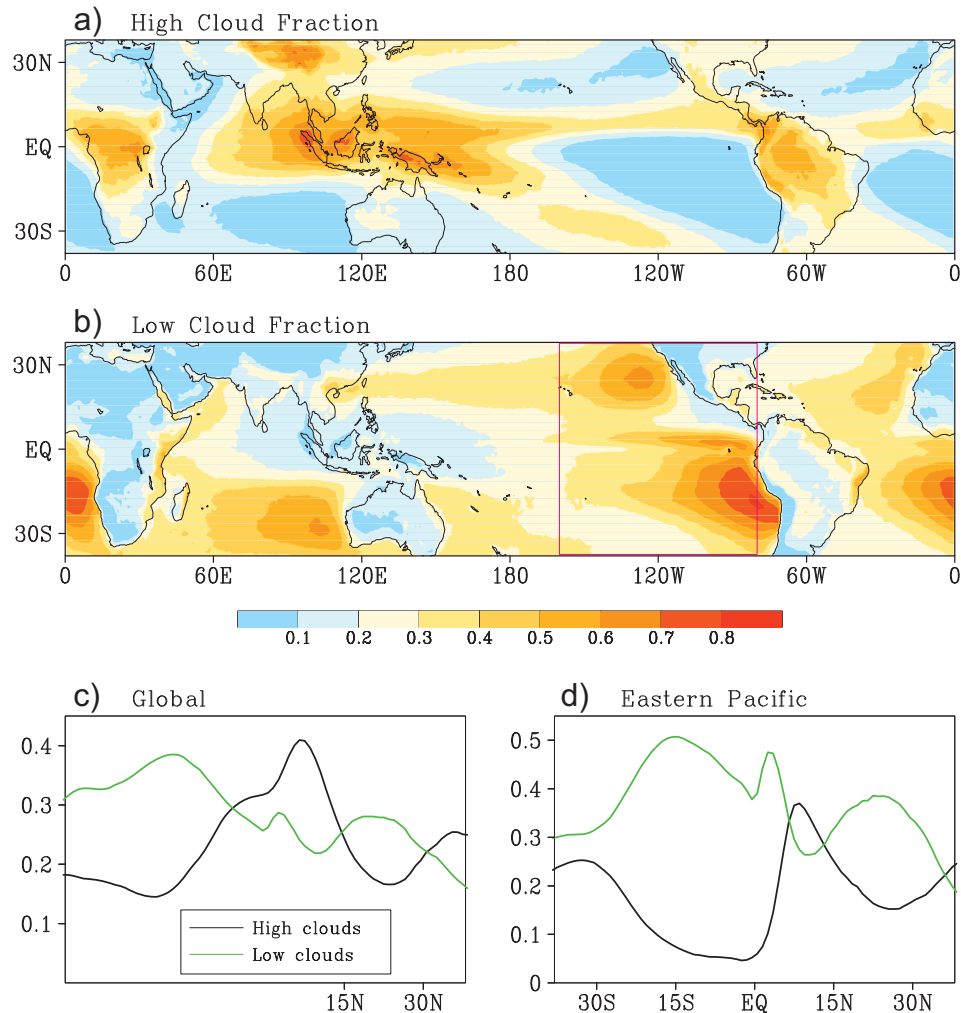
The time-latitude rainfall anomaly diagram for the Indian p0070 Ocean region (9b) shows variability quite different than that exhibited by the ITCZ over Africa. First, the meridional extent of the anomalous excursions is much greater, extending to at least  $30^\circ$ . For the most part, this is simply related to the much broader latitudinal extent of the mean ITCZ pattern in this region (i.e., Figures 2 and 8). Second, the intensity of the fluctuations is slightly greater, ranging up to about  $\pm 3\text{ mm day}^{-1}$ . However, given the larger mean rainfall values for this region, this anomaly range represents deviations from the annual cycle on the order of 25% which is similar to the case for Africa. Third, even with the seasonal smoothing applied to the data, the ITCZ in this region exhibits considerably more variability at shorter time scales than for example the ITCZ over Africa. This shorter term variability is partly attributable to the Intraseasonal Oscillation that has been found to prevail most strongly over the Indian and western Pacific Oceans. Given the distribution of land and people within this sector, the most consequential of the rainfall anomalies occur in the Northern Hemisphere summer, north of about  $15^\circ\text{ N}$ . From Figure 7, it can be seen that the maximum rainfall associated with the Indian summer monsoon occurs in July. Figure 8(b) illustrates some aspects of the variability associated with the timing and strength of the Asian monsoon as it relates to the ITCZ. For example, in 1980, the rainfall associated with the northward migration of the ITCZ and the development of the summer monsoon was particularly intense, while the 1981 summer monsoon appears to have come slightly earlier than normal. In contrast, the summer monsoons of 1983, 1987, and 1989 are examples of the monsoon-related ITCZ rainfall being a bit weaker than normal. It is important to emphasize out that even though these anomalies ( $\sim 1\text{ mm day}^{-1}$ ) only represent about 10% of the total rainfall that typically occurs during the monsoon (Figure 8(b)), they represent very important departures for the people and industries (e.g., agriculture) that are affected by them.

For the case of the central Pacific (9c), the anomalous ITCZ p0075 rainfall is dominated by negative and positive anomalies on or

f0050 **Figure 9**

near the equator. Note that these values are significantly larger than the ITCZ rainfall anomalies occurring in either of the other longitude sectors discussed above (including those longitude sectors not discussed). In this region, the zonally averaged rainfall anomalies range up to at least  $\pm 7$  mm day<sup>-1</sup>. In some instances, particularly for the large anomalies right on the equator, these values can exceed 100% of the mean values associated with the annual cycle (Figure 7(d)). These large variations in the position and intensity of the ITCZ in this region are associated with climate phenomena known as the El Niño – Southern Oscillation (ENSO). In warm phases of ENSO (i.e., El Niño), SST in the central and eastern equatorial Pacific

Ocean can become anomalously warm by about 1–3 °C, while in cold phases (i.e., La Niña), this region becomes anomalously cool by a similar magnitude. This has a dramatic effect on the organization of tropical convection in this region as well as in regions remote to the central Pacific. Evident from Figure 9(c) are the large positive rainfall anomalies associated the strong El Niño of 1982–83, moderate El Niño of 1986–87, and the prolonged and somewhat weaker El Niño(s) of the early 1990s. Typically, these events cause the two convergence zones which are located slightly away from the equator in the central Pacific to merge into a single zone of convection and rainfall centered on or very near the equator. The large negative equatorial

f0055 **Figure 10**

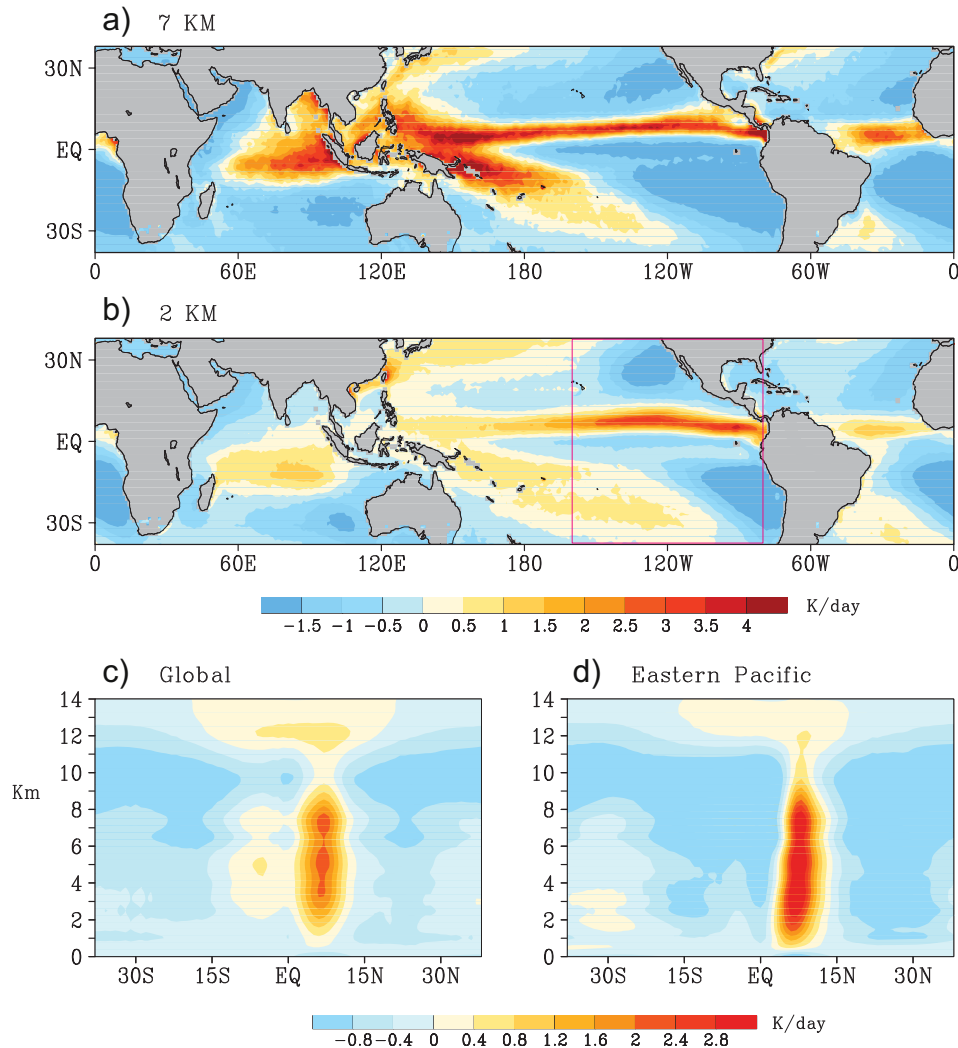
rainfall anomalies are associated with the La Ninas of 1984, 1988–89, and 1995–96. Central Pacific rainfall anomalies associated with La Nina typically cause the relatively dry equatorial zone near the dateline (Figure 2) to become even drier and to extend further west than normal. It is important to point out that these central Pacific ENSO-related ITCZ rainfall anomalies do not occur in isolation. Typically, these anomalies induce anomalies of the opposite sense and a somewhat weaker magnitude in the western Pacific sector and in some cases the Indian Ocean and South American sectors as well. In fact, these ENSO-related rainfall anomalies are so large, that they are the only significant departure that appears to occur in the global mean ITCZ (data not shown). Anomalies in the global mean ITCZ rainfall are typically in phase with the anomalies in the central and eastern Pacific Ocean and have magnitudes that range up to about  $1 \text{ mm day}^{-1}$ . However, with respect to quantifying the size of this climate signal in the context of the ITCZ, it is important to point out that accurate measurements of rainfall over the oceanic regions are possible only with satellite retrievals and this is still an area of active research.

### Perspectives from New Satellite Observations

Recently launched satellite instruments provide an unprecedented opportunity to characterize the three-dimensional structure of the ITCZ. Figure 10 depicts the long-term mean distribution of high and low cloud fractions derived from the Moderate Resolution Imaging Spectroradiometer (MODIS) instrument. The pattern of high cloud fractions (Figure 10(a)) largely follows the mean rainfall pattern in Figure 2, suggesting the development of deep convective clouds within the ITCZ. Meanwhile, low clouds prevail over subtropical regions over the eastern Pacific and Atlantic Oceans as well as in the southern Indian Ocean (Figure 10(b)). Maximum low cloud fractions are exhibited over the eastern portions of these ocean basins, largely due to coastal oceanic upwelling induced by the trade winds and downward motion in the subtropical high region associated downward branch of the Hadley Circulation (Figure 7). Meridional asymmetry in cloud fraction about the equator is clearly evident in Figure 10(c) and 10(d). Maximum deep cloud fractions are found near  $6^\circ \text{ N}$  in the globally zonal mean profile (Figure 10(c)), largely representing

s0030

p0080

f0060 **Figure 11**

the northward displaced ITCZ over the eastern Pacific and Atlantic Oceans. Meanwhile, minimum high cloud fractions are observed over the subtropical latitudes in both hemispheres, where the maxima in low cloud fractions are evident. In addition to the two peaks over the subtropical regions in both hemispheres, there is a third maximum of low cloud fraction found just north of the equator, which captures the low cloud maximum over the eastern Pacific at this latitude belt (see [Figure 10\(b\)](#)). Similar features in high and low cloud profiles are found over the eastern Pacific sector ([Figure 10\(d\)](#)). High clouds are largely confined within a narrow latitude belt centered at  $9^\circ$  N. Over the broad region on both sides of the ITCZ, low clouds dominate whereas high clouds are largely suppressed.

p0085 [Figure 11](#) displays spatial distribution of long-term mean total atmospheric diabatic heating at 7 and 2 km as well as its height-latitude profiles averaged over the global longitudes and eastern Pacific sectors. These heating fields are derived based on the measurements from microwave imager and precipitation radar aboard the Tropical Rainfall Measurement Mission

(TRMM). The heating pattern at 7 km largely mirrors the mean rainfall pattern in [Figure 2](#), suggesting the dominance of the condensational latent heating release in the total diabatic heating over these tropical convective regions. In convectively inactive regions, over regions where low clouds dominate ([Figure 10\(b\)](#)) in particular, the total diabatic heating at 7 km is characterized by strong net cooling due to the radiative heat loss in the absence of deep clouds. At 2 km, while strong radiative cooling is still evident over these low cloud regions, heating over the convective regions generally exhibits weaker amplitude compared to that at 7 km. A weak heating center is found over the southern Indian Ocean near  $10^\circ$  S at 2 km, in contrast to the maximum heating near the equator and northern Indian Ocean at 7 km.

The deep structure of the convection over the ITCZ regions is p0090 further evident in [Figure 11\(c\)](#), which illustrates the globally averaged mean vertical-latitude diabatic heating profiles. A strong heating maximum is observed to the north of the equator centered at  $8^\circ$  N, stretching from lower troposphere to upper level near 10 km. Another relatively weaker heating

center is found to the south of equator near  $5^{\circ}$  S, reflecting the condensational heating release over the SPCZ and ITCZ over the Indian Ocean. The heating amplitude over the southern branch is much weaker than its counterpart in northern hemisphere, largely due to the inclusion of the cold SST tongue regions over the eastern Pacific and Atlantic Oceans in the global averages. The strong deep heating structure coupled with the ITCZ convection over the eastern Pacific is further displayed in [Figure 11\(d\)](#), with broad cooling regions present on both sides of the heating area. The strong vertically developed heating over the ITCZ is crucial in driving the atmospheric circulation, which in turn plays a central role in the global water and energy cycles as depicted in [Figure 7](#).

*See also:* Air-Sea Interaction; Boundary Layers; 00307; Dynamic Meteorology; 00161; Hurricanes; Instability; Conditional/Convective; Monsoon; Ocean Circulation; 00415; El Nino – Southern Oscillation.

### Further Reading

- Emanuel, K.A., 1994. Atmospheric Convection. Oxford University Press, New York.  
Gill, A.E., 1982. Atmosphere-Ocean Dynamics. Academic Press, Orlando, FL.  
Henderson-Sellers, A., Robinson, P.J., 1986. Contemporary Climatology. Longman Scientific and Technical, Essex, UK.  
Houghton, J.T., 1986. The Physics of the Atmosphere. Cambridge University Press, Cambridge, UK.  
Kidder, S.Q., Vonder Haar, T.H., 1995. Satellite Meteorology: An Introduction. Academic Press, San Diego, CA.  
Kraus, E.B., Businger, J.A., 1994. Atmosphere-Ocean Interaction. Oxford University Press, New York.  
Lindzen, R.S., 1990. Dynamics in Atmospheric Physics. Cambridge University Press, Cambridge, UK.  
Salby, M.L., 1996. Fundamentals of Atmospheric Physics. Academic Press, San Diego, CA.